

# Ocean oxygenation in the wake of the Marinoan glaciation

Swapan K. Sahoo<sup>1</sup>, Noah J. Planavsky<sup>2</sup>, Brian Kendall<sup>3</sup>†, Xinqiang Wang<sup>4</sup>, Xiaoying Shi<sup>4</sup>, Clint Scott<sup>5</sup>, Ariel D. Anbar<sup>3,6</sup>, Timothy W. Lyons<sup>2</sup> & Ganqing Jiang<sup>1</sup>

**Metazoans are likely to have their roots in the Cryogenian period<sup>1–3</sup>, but there is a marked increase in the appearance of novel animal and algae fossils shortly after the termination of the late Cryogenian (Marinoan) glaciation about 635 million years ago<sup>4–6</sup>. It has been suggested that an oxygenation event in the wake of the severe Marinoan glaciation was the driving factor behind this early diversification of metazoans and the shift in ecosystem complexity<sup>7,8</sup>. But there is little evidence for an increase in oceanic or atmospheric oxygen following the Marinoan glaciation, or for a direct link between early animal evolution and redox conditions in general<sup>9</sup>. Models linking trends in early biological evolution to shifts in Earth system processes thus remain controversial<sup>10</sup>. Here we report geochemical data from early Ediacaran organic-rich black shales (~635–630 million years old) of the basal Doushantuo Formation in South China. High enrichments of molybdenum and vanadium and low pyrite sulphur isotope values ( $\Delta^{34}\text{S}$  values  $\geq 65$  per mil) in these shales record expansion of the oceanic inventory of redox-sensitive metals and the growth of the marine sulphate reservoir in response to a widely oxygenated ocean. The data provide evidence for an early Ediacaran oxygenation event, which pre-dates the previous estimates for post-Marinoan oxygenation<sup>11–13</sup> by more than 50 million years. Our findings seem to support a link between the most severe glaciations in Earth's history, the oxygenation of the Earth's surface environments, and the earliest diversification of animals.**

The increase of oxygen in Earth's surface environments was protracted and is thought to have proceeded in two major steps. The ocean–atmosphere system was essentially devoid of oxygen until very early in the Proterozoic eon, when atmospheric oxygen rose to  $>1\%$  of the present atmospheric level (PAL)<sup>14,15</sup>. The timing and dynamics of this initial oxygenation are under active investigation, but there is little doubt that a major atmospheric transition, the 'Great Oxidation Event' (GOE), occurred about 2.4 billion years (Gyr) ago<sup>14,15</sup>. It is commonly assumed that there was a second significant oxygen rise to near PAL during the late Neoproterozoic (~750–542 Myr ago)<sup>14,15</sup>; however, the timing and magnitude of this second oxygenation event remain elusive<sup>9,15</sup>.

The appearance of metazoan fossils has traditionally been used as a minimum estimate for the timing of the late Neoproterozoic oxygenation event<sup>16</sup>. Molecular clock estimates place the origin of crown-group animals in the Cryogenian period (850–635 Myr ago)<sup>1</sup>. There are also sponge biomarkers<sup>2</sup> and sponge-like fossils<sup>3</sup> in Cryogenian or older rocks, but these are only simple metazoans with limited oxygen demands (see Supplementary Information). Novel micro- and macrofossils interpreted as early metazoans appear immediately above Marinoan-age (~635 Myr ago) glacial deposits in South China<sup>4–6</sup> (see Supplementary Information). Further, there is a radiation in marine algae following the Marinoan glaciation, which is probably linked to a

metazoan-driven shift in trophic structure and ecosystem complexity<sup>17</sup>. It has been proposed that this biological innovation is linked to an oxygenation event following the extensive Marinoan glaciation<sup>7,8</sup>. However, there is no direct geochemical evidence for an increase in ocean oxygenation in the immediate aftermath of the Marinoan glaciation. Most existing geochemical evidence for a late Neoproterozoic redox shift is much younger (~580–550 Myr old), controversial, or records a local shift in redox conditions that may not be globally representative<sup>9,11–13</sup>.

Trace-metal enrichments in black shales can record information about the global ocean redox state<sup>13,18–20</sup>. Following the establishment of pervasive oxidative weathering after the GOE at ~2.4 Gyr ago<sup>14,15</sup>, the size of the global marine reservoir of redox-sensitive elements (RSEs) was primarily controlled by the spatial extent of anoxic versus oxic marine conditions<sup>18,19</sup>. In reducing marine environments, the burial fluxes of many RSEs, notably molybdenum (Mo) and vanadium (V), exceed those in oxygenated settings by several orders of magnitude. Hence, it follows that when oxic conditions are more widespread, the global seawater concentrations of these RSEs will be higher<sup>18</sup>. For example, in today's predominantly oxygenated oceans, Mo is the most abundant transition metal (~105 nM; ref. 18), despite its very low crustal abundance (~1 p.p.m.; ref. 21). Because the residence time of Mo (800–440 kyr)<sup>18,22</sup> and V (~50 kyr)<sup>18</sup> in seawater is much longer than the ocean mixing time (~1.5 kyr), Mo and V in marine basins track the global average conditions<sup>18–20,22</sup>. This concept is well-grounded in an understanding of the modern Mo and V global mass balances<sup>18,19</sup>.

The magnitude of RSE enrichments in anoxic marine sediments reflect dissolved RSE concentrations in seawater<sup>20,23</sup>. In general, RSE enrichments also scale with the organic carbon flux because reduced, particle-reactive metal species (for example, thiomolybdate or vanadyl ions) are bound by organic particles, resulting in strong correlations between the metal and total organic carbon (TOC) contents in modern anoxically deposited sediments and black shales<sup>20,23</sup>. Therefore, authigenic enrichments are commonly normalized to TOC concentrations (for example, Mo/TOC and V/TOC)<sup>23</sup>. RSE enrichments in anoxic shales may also depend on other factors, such as sedimentation rates and sulphide levels. However, studies in modern anoxic basins with access to the open ocean<sup>18–20,23</sup> have shown that the dissolved metal concentrations exert a first-order control on the degree of the enrichment (see Supplementary Information). This relationship sets the stage for using RSE enrichments in anoxic shales to track Earth's oxygenation history and specifically the extents of anoxia in the ocean<sup>9,13,23</sup>.

The temporal record of RSE enrichments in shales deposited beneath an anoxic water column currently provides the least controversial and most direct geochemical signal for a significant redox shift in the late Neoproterozoic<sup>9,13</sup>. However, the existing data only show a jump in RSE enrichments to Phanerozoic values near the end of the Ediacaran

<sup>1</sup>Department of Geoscience, University of Nevada, Las Vegas, Nevada 89154, USA. <sup>2</sup>Department of Earth Sciences, University of California, Riverside, California 92521, USA. <sup>3</sup>School of Earth and Space Exploration, Arizona State University, Tempe, Arizona 85287, USA. <sup>4</sup>School of Earth Science and Resources, China University of Geosciences, Beijing 10008, China. <sup>5</sup>Department of Earth and Planetary Sciences, McGill University, Montreal, Quebec H3A 2A7, Canada. <sup>6</sup>Department of Chemistry and Biochemistry, Arizona State University, Tempe, Arizona 85287, USA. †Present address: Department of Earth and Environmental Sciences, University of Waterloo, Waterloo, Ontario N2L 3G1, Canada.

period (~551 Myr ago)<sup>9,13,24</sup>, long after the radiation of complex metazoans including triploblastic animals<sup>4–6,25</sup>. There is a pronounced data gap between this time and 663 Myr ago in previous analyses due to the lack of suitable open-marine, deep-water black shale samples<sup>9,13</sup>. Here we fill this gap by analysing organic-rich black shales of the basal Doushantuo Formation in South China that were probably deposited between 635 and 630 Myr ago (see Supplementary Information). We found very high, Phanerozoic-like RSE enrichments within a few million years after the Marinoan glaciation, coincident with the appearance of the earliest non-poriferan metazoan fossils<sup>4,5</sup>.

In South China, Marinoan-age glacial diamictites of the Nantuo Formation are overlain by a 3-to-6-m thick,  $635.2 \pm 0.6$  Myr old<sup>26</sup> cap carbonate commonly referred to as Member I of the Doushantuo Formation (Fig. 1)<sup>27</sup>. The cap carbonate is conformably overlain by organic-rich black shales (Member II of the Doushantuo Formation), with subordinate carbonate layers and phosphorite-chert nodules in shelf and upper-slope environments<sup>27</sup> (see Supplementary Information). Putative metazoan fossils were found 6 m above the Doushantuo cap carbonate in the Yangtze Gorges area<sup>4,5</sup>, less than two metres above an ash bed that has been dated as  $632.5 \pm 0.5$  Myr old<sup>26</sup>. Morphologically complex macroscopic fossils of the Lantian biota<sup>6</sup> were reported from slope-basinal black shales, approximately 15 m above the cap carbonate (Fig. 1). Our geochemical analyses focus on the basal Member II black shales, which are roughly equivalent or slightly below these fossil horizons.

The basal Member II black shales have a transitional contact with the underlying cap carbonate<sup>28</sup>. Their widespread occurrence across the basin and lack of event beds (for example, turbidites and olistostromes) suggest that they were deposited during the latest stage of postglacial transgression or sea-level highstand, with the shelf-to-basin topography inherited from the Cryogenian<sup>27</sup> (see Supplementary Information). We focused on deepwater Member II samples collected from three sections in an open-marine, slope/basinal setting (Fig. 1 and Supplementary Fig. 1). The black shales in the lower slope and basin sections contain an average of ~2.0 wt% of both pyrite iron ( $\text{Fe}_{\text{pyrite}}$ ) and total organic carbon (TOC). The upper slope section has comparatively lower  $\text{Fe}_{\text{pyrite}}$  (~0.3 wt% on average) and higher TOC (2.3 wt% on average); see Supplementary Table 1.

Slope and basin post-glacial black shales of Member II show strong Mo and V enrichments (Fig. 2). Mo enrichments in these sections commonly exceed the average Phanerozoic euxinic (anoxic and sulphidic) shale concentration of ~100 p.p.m. and the Phanerozoic

average Mo/TOC ratio (p.p.m./wt%) of ~25 (refs 9, 13). These high Mo enrichments show that the local water column was not only anoxic but also had free dissolved sulphide (euxinic conditions)<sup>23</sup>. Vanadium enrichments of several thousand p.p.m. are common and equivalent to the largest values observed in the Phanerozoic anoxic shale record<sup>9</sup> (Fig. 3). Similarly, uranium (U) in the lower Doushantuo Formation (Fig. 2) exceeds 30 p.p.m.—equivalent to the largest enrichments observed in modern anoxic basins<sup>29</sup>. Therefore, the magnitude of RSE enrichments used previously to argue for a late Neoproterozoic oxygenation event at ~551 Myr ago<sup>9,13</sup> are now found in >630-Myr-old, early Ediacaran black shales (Fig. 3). It is well established that basin restriction, if anything, decreases the extent of RSE enrichment<sup>20,23</sup>, ruling out the possibility that the large enrichments have only local significance (see Supplementary Information). Also, other factors, such as persistent or transient occurrences of oxygen in overlying waters, consistently mute the magnitude of RSE enrichment<sup>23</sup>. Hence, the large RSE enrichments in the lower Doushantuo Formation provide strong evidence for a significant global marine oxygenation event in the aftermath of the Marinoan glaciation.

Simple mass-balance calculations confirm that the observed Mo and V enrichments in the lower Doushantuo Formation require a well-oxidized ocean (see Supplementary Information). Building from the global Mo and V cycles<sup>18,19</sup>, it is possible to estimate the effects of increasing riverine RSE flux on the marine Mo and V reservoirs. Even with a very elevated riverine flux of Mo and V, the marine redox landscape will control RSE reservoir sizes and thus RSE enrichments. For instance, based on mass-balance calculations, even a doubling of the riverine Mo or V flux can be compensated for by relatively small growth in the extent of euxinia (for example, 1–2% of the seafloor area; see Supplementary Fig. 3). Although continental Mo and V fluxes may have been elevated for short periods (thousands of years) during the most rapid stages of glacial retreat, glacially elevated fluxes are not expected during deposition of the examined black shales, which span a period of millions of years after glacial retreat. Mass-balance calculations also indicate that even a relatively small areal increase (for example, 2–3%) in anoxic seafloor would crash the Mo and V reservoirs on a timescale of  $\leq 0.5$  Myr (see Supplementary Information). Thus, the observed Mo and V enrichments in lower Doushantuo Formation black shales suggest that oxic waters bathed the vast majority of the ocean. Oxygen-deficient conditions must have been spatially limited and only located where high organic matter loading caused oxygen depletion along ocean margins, such as in the Nanhua basin.

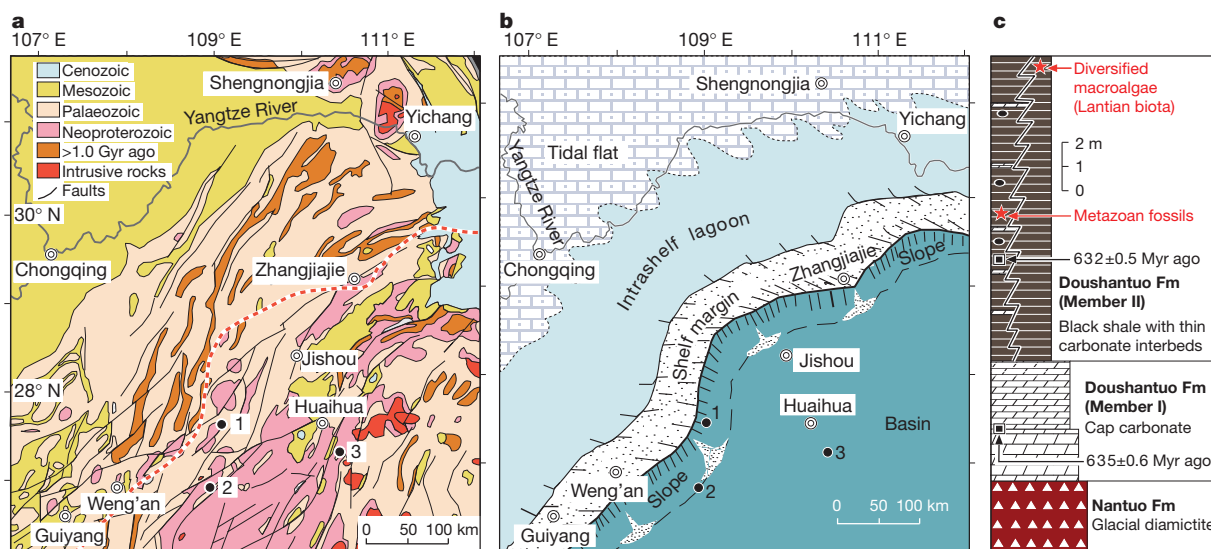


**Figure 1** | Local maps and stratigraphy. **a**, Simplified geological map with location of sections (1, Taoying; 2, Wuhe; 3, Yuanjia). The dashed red line marks the shelf margin during deposition of the Doushantuo Formation.

**b**, Palaeogeographic model for the Doushantuo Formation (simplified from ref. 27). **c**, Stratigraphy of the lower Doushantuo Formation with radiometric ages<sup>26</sup> and important fossil horizons<sup>4–6</sup> marked.

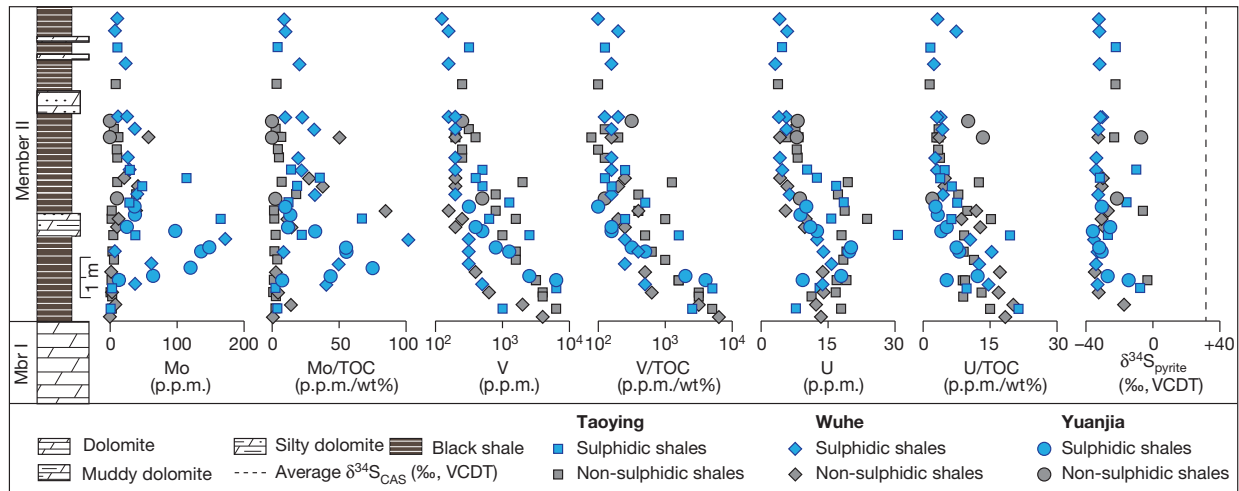


**Figure 2 | Trace-metal abundances (Mo, Mo/TOC, V, V/TOC, U, U/TOC) and pyrite sulphur isotopes ( $\delta^{34}\text{S}_{\text{pyrite}}$ ) from the lower Doushantuo Formation black shales.**

The shape of the data symbols indicates sample locations: Taoying (upper-slope section; squares), Wuhe (lower-slope section; diamonds), and Yuanjia (basin section; circles). The colour of the data symbols is used to distinguish sulphidic ( $\text{Fe}_{\text{pyrite}}/\text{Fe}_{\text{HR}} > 0.8$ ; grey) from non-sulphidic ( $\text{Fe}_{\text{pyrite}}/\text{Fe}_{\text{HR}} < 0.8$ ; light green) shales (Supplementary Fig. 2). Because a large

Large variability in the magnitude of RSE enrichments in lower Doushantuo Formation black shales suggests locally variable redox conditions. There are intervals with high RSE enrichments adjacent ( $< 0.2$  m) to intervals with near-crustal, un-enriched RSE concentrations, despite apparently constant physical conditions (that is, absence of wave-, storm- and gravity-generated beds) well below the storm wave base (see Supplementary Information). These variations suggest significant redox shifts in environments and thus deposition of the units under mixed oxic, suboxic-ferruginous, and euxinic conditions. Redox fluctuations in deep-water environments well below the mixed

portion of the Doushantuo samples have unusually low total iron ( $\text{Fe}_{\text{T}}$ )/aluminium (Al) ratios (Supplementary Table 1), we do not use highly reactive iron ( $\text{Fe}_{\text{HR}}$ )/total iron ( $\text{Fe}_{\text{T}}$ ) ratios as a quantitative palaeoredox proxy (see Supplementary Information). The dashed line in the  $\delta^{34}\text{S}_{\text{pyrite}}$  panel marks the average  $\delta^{34}\text{S}_{\text{CAS}}$  value of the analysed stratigraphic interval<sup>5,24</sup>. Sulphur isotope data are reported as per mil (‰) deviations from the isotope composition of Vienna Cañon Diablo Troilite (VCDT).

layer, including those at an estimated depth of  $> 1,000$  m in the basinal section<sup>27,28</sup> (see Supplementary Information), are consistent with a well-oxygenated global ocean–atmosphere system.

All Mo, V and U concentrations shift to lower values in the upper part of the basal Doushantuo black shales (Fig. 2). Given the observed variability in RSE enrichments within the basal unit, this drop in RSE enrichments may record a local environmental shift towards less reducing conditions that are not conducive to redox-sensitive metal sequestration (see Supplementary Information). Alternatively, the decrease of RSE values may record a shift back to more reducing ocean conditions

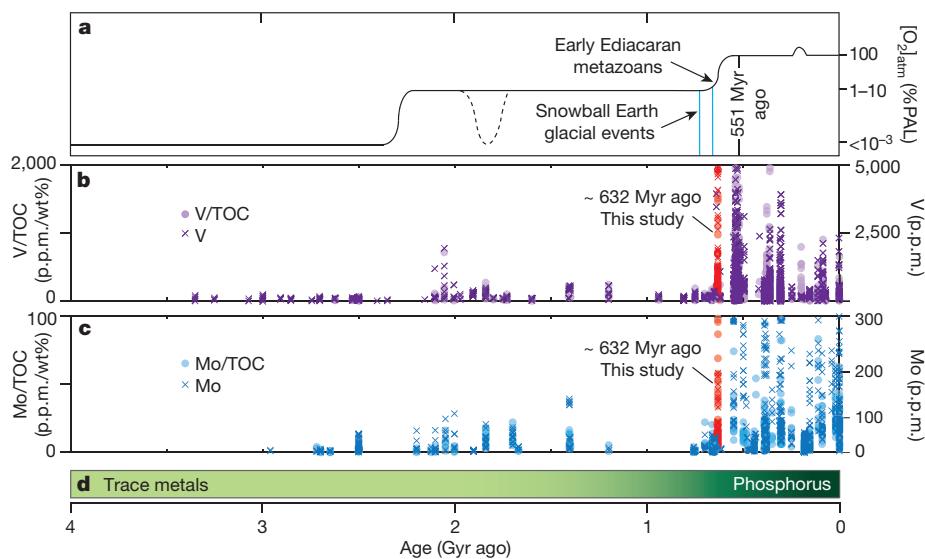


**Figure 3 | Summary of redox-sensitive trace elements and evolution of the ocean–atmosphere redox state.** **a**, Atmospheric oxygen levels compared with present atmospheric level (PAL). The early Ediacaran metazoans<sup>4,5</sup> appeared shortly after the Marinoan glaciation, during an increase in ocean–atmosphere oxygen level (modified from ref. 8). **b**, Temporal trends in V enrichments (crosses) and V/TOC ratios (circles) in euxinic black shales (Supplementary Tables 2 and 3). **c**, Temporal trends in Mo enrichments (crosses) and Mo/TOC ratios (circles) in euxinic black shales (Supplementary Tables 2 and 3). The spikes of V, V/TOC, Mo and Mo/TOC from the lower Doushantuo black shales (this study) are marked. **d**, Potential shift in nutrient-limiting factor from trace metals

to phosphorus after the Marinoan glaciation<sup>8,32</sup>. Data compilation, stratigraphic and chronological details are provided in the Supplementary Information. The Mo and V records indicate that the ocean experienced a late Neoproterozoic growth in the inventory of redox-sensitive trace elements, which can be linked to ocean ventilation. This redox shift was previously thought to have occurred at  $\sim 551$  Myr ago<sup>9,13</sup>. Our study provides evidence for an oxygenation event associated with increased seawater Mo–V enrichments and Mo/TOC and V/TOC ratios in the aftermath of the Marinoan glaciation, synchronous with or slightly pre-dating the earliest non-poriferan metazoan fossil record at  $\sim 632$  Myr ago.

typical of the mid-Proterozoic (~1,800–700 Myr ago)—implying that the early Ediacaran oxygenation was not a unidirectional process (see Supplementary Information). However, this possibility requires a more comprehensive test in broader palaeogeographic settings of the Nanhua basin and in other global successions.

Highly negative pyrite sulphur isotope ( $\delta^{34}\text{S}_{\text{pyrite}}$ ) values down to  $-35\%$  from the basinal samples (Fig. 2; Supplementary Table 1) further support our interpretation of an oxygenated ocean–atmosphere system following Marinoan deglaciation. Coeval (~635–630 Myr) carbonate-associated sulphate sulphur isotope ( $\delta^{34}\text{S}_{\text{CAS}}$ ) values from shelf sections<sup>5,24</sup> have an average of  $\sim 34\%$ . In this framework, the calculated isotope fractionation between pyrite and coeval sulphate ( $\Delta^{34}\text{S}$ ) in the deep basin section is  $>65\%$ —equivalent to maximum fractionations by modern sulphate reducing bacteria<sup>30</sup> and the maximum pyrite–coeval sulphate offset observed in the Phanerozoic rock record<sup>9,31</sup> (Supplementary Fig. 4). An increase in the isotopic offset between pyrite and seawater sulphate in the late Neoproterozoic has been commonly linked to growth of the global marine sulphate reservoir and surface oxidation<sup>9,31</sup>. The large sulphur isotope fractionation in the basal Member II shales therefore points towards a pervasively oxygenated ocean with lower associated pyrite burial, consistent with the conclusion drawn from RSE enrichments.

The shift to pervasively oxygenated oceans and, by inference, higher atmosphere  $\text{O}_2$  conditions following the Marinoan glaciation may be linked to high nutrient availability<sup>8</sup>. It has been proposed that there was a large marine phosphate reservoir during and following the Cryogenian glacial events<sup>7,8</sup>. Phosphate is commonly considered as the ultimate limiting nutrient on geological timescales, as nitrogen (N) can be supplied by biological nitrogen fixation from an essentially limitless atmospheric supply. Therefore, glacially induced perturbations to the phosphorus cycle may have triggered an organic carbon burial event<sup>28</sup> that induced a shift towards higher oxygen levels.

This model, however, overlooks the potential for persistent N stress linked to trace-metal biolimitation<sup>32</sup>. In a broadly anoxic ocean, chalcophilic trace metals (for example, Mo, Cu, Cd) may be co-limiting nutrients and inhibit efficient N fixation—just as in the modern oxic marine system Fe stress limits N fixation over broad swaths of the ocean<sup>32</sup>. Significant Mo biolimitation may have limited the organic carbon production and stabilized the redox state of the oceans through the mid-Proterozoic<sup>32</sup>. In this light, a jump in sulphidic black shale Mo enrichments at the Cryogenian–Ediacaran transition probably records a shift in nutrient regimes as well as in global redox conditions.

Marine chalcophilic trace-metal levels following glacial retreat must have been sufficient to allow for significant organic carbon burial and the switch to a more pervasively oxygenated ocean. Dissolved marine Mo may have built up to the critical levels needed to move out of a marine system with chronic Mo-induced N stress during glaciation. A brief episode (for example, thousands of years) of increased Mo delivery associated with high rates of postglacial weathering before the deposition of the Doushantuo Member II shales may have also helped to provide the perturbation needed to overcome persistent Mo biolimitation. Mitigating coupled Mo–N stress would have allowed for efficient utilization of a large marine phosphate reservoir<sup>7,8</sup>—ultimately promoting organic carbon burial and oxygen release. Ventilation of the ocean would lead to significant growth of the Mo reservoir (and other RSE reservoirs) as manifest in the Member II shales deposited several million years after glacial retreat. The formerly enigmatic association of the ‘Snowball Earth’ glaciations and early metazoan and algal diversification could thus be linked to shifts in nutrient availability, burial of organic carbon, and ultimately the shift to a more oxygenated ocean–atmosphere system that favoured the early diversification of metazoan life and ecosystems.

Received 3 March; accepted 26 July 2012.

1. Erwin, D. H. *et al.* The Cambrian conundrum: early divergence and later ecological success in the early history of animals. *Science* **334**, 1091–1097 (2011).

2. Love, G. D. *et al.* Fossil steroids record the appearance of Demospongiae during the Cryogenian period. *Nature* **457**, 718–721 (2009).
3. Maloof, A. C. *et al.* Possible animal-body fossils in pre-Marinoan limestones from South Australia. *Nature Geosci.* **3**, 653–659 (2010).
4. Yin, L. *et al.* Doushantuo embryos preserved inside diapause egg cysts. *Nature* **446**, 661–663 (2007).
5. McFadden, K. A. *et al.* Pulsed oxidation and biological evolution in the Ediacaran Doushantuo Formation. *Proc. Natl Acad. Sci. USA* **105**, 3197–3202 (2008).
6. Yuan, X. *et al.* An early Ediacaran assemblage of macroscopic and morphologically differentiated eukaryotes. *Nature* **470**, 390–393 (2011).
7. Hoffman, P. F. & Schrag, D. P. The snowball Earth hypothesis: testing the limits of global change. *Terra Nova* **14**, 129–155 (2002).
8. Planavsky, N. J. *et al.* The evolution of the marine phosphate reservoir. *Nature* **467**, 1088–1090 (2010).
9. Och, L. M. & Shields-Zhou, G. A. The Neoproterozoic oxygenation event: environmental perturbations and biogeochemical cycling. *Earth Sci. Rev.* **110**, 26–57 (2012).
10. Butterfield, N. J. Oxygen, animals and oceanic ventilation: an alternative view. *Geobiology* **7**, 1–7 (2009).
11. Fike, D. A. *et al.* Oxidation of the Ediacaran ocean. *Nature* **444**, 744–747 (2006).
12. Canfield, D. E., Poulton, S. W. & Narbonne, G. M. Late-Neoproterozoic deep-ocean oxygenation and the rise of animal life. *Science* **315**, 92–95 (2007).
13. Scott, C. *et al.* Tracing the stepwise oxygenation of the Proterozoic ocean. *Nature* **452**, 456–459 (2008).
14. Holland, H. D. The oxygenation of the atmosphere and oceans. *Phil. Trans. R. Soc. B* **361**, 903–915 (2006).
15. Canfield, D. E. The early history of atmospheric oxygen: homage to Robert A. Garrels. *Annu. Rev. Earth Planet. Sci.* **33**, 1–36 (2005).
16. Knoll, A. H. & Carroll, S. E. Early animal evolution: emerging views from comparative biology and geology. *Science* **284**, 2129–2137 (1999).
17. Peterson, K. J. & Butterfield, N. J. Origin of the Eumetazoa: testing ecological predictions of molecular clocks against the Proterozoic fossil record. *Proc. Natl Acad. Sci. USA* **102**, 9547–9552 (2005).
18. Emerson, S. R. & Huested, S. S. Ocean anoxia and the concentrations of molybdenum and vanadium in seawater. *Mar. Chem.* **34**, 177–196 (1991).
19. Hastings, D. W., Emerson, S. R. & Mix, A. C. Vanadium in foraminiferal calcite as a tracer for changes in the areal extent of reducing sediments. *Paleoceanography* **11**, 665–678 (1996).
20. Algeo, T. J. & Lyons, T. W. Mo-total organic carbon covariation in modern anoxic marine environments: implications for analysis of paleoredox and paleohydrographic conditions. *Paleoceanography* **21**, PA1016, <http://dx.doi.org/10.1029/2004PA001112> (2006).
21. Wedepohl, K. H. The composition of the continental crust. *Geochim. Cosmochim. Acta* **59**, 1217–1232 (1995).
22. Miller, C. A., Peucker-Ehrenbrink, B., Walker, B. D. & Marcantonio, F. Re-assessing the surface cycling of molybdenum and rhenium. *Geochim. Cosmochim. Acta* **75**, 7146–7179 (2011).
23. Lyons, T. W. *et al.* Tracking euxinia in the ancient ocean: a multiproxy perspective and Proterozoic case study. *Annu. Rev. Earth Planet. Sci.* **37**, 507–534 (2009).
24. Li, C. *et al.* A stratified redox model for the Ediacaran ocean. *Science* **328**, 80–83 (2010).
25. Pecoits, E. *et al.* Bilateral burrows and grazing behavior at >585 million years ago. *Science* **336**, 1693–1696 (2012).
26. Condon, D. *et al.* U–Pb ages from the Neoproterozoic Doushantuo Formation, China. *Science* **308**, 95–98 (2005).
27. Jiang, G. *et al.* Stratigraphy and paleogeography of the Ediacaran Doushantuo Formation (ca. 635–551 Ma) in South China. *Gondwana Res.* **19**, 831–849 (2011).
28. Jiang, G. *et al.* Organic carbon isotope constraints on the dissolved organic carbon (DOC) reservoir at the Cryogenian–Ediacaran transition. *Earth Planet. Sci. Lett.* **299**, 159–168 (2010).
29. Calvert, S. E. & Pedersen, T. F. Geochemistry of recent oxic and anoxic marine sediments: implications for the geological record. *Mar. Geol.* **113**, 67–88 (1993).
30. Sim, M. S., Bosak, T. & Ono, S. Large sulfur isotope fractionation does not require disproportionation. *Science* **333**, 74–77 (2011).
31. Canfield, D. E. & Raiswell, R. The evolution of the sulfur cycle. *Am. J. Sci.* **299**, 697–723 (1999).
32. Anbar, A. D. & Knoll, A. H. Proterozoic ocean chemistry and evolution: a bioinorganic bridge? *Science* **297**, 1137–1142 (2002).

Supplementary Information is available in the online version of the paper.

**Acknowledgements** This study was supported by the National Science Foundation Division of Earth Science, NASA Astrobiology programme and National Natural Science Foundation of China. We are grateful to S. Xiao for input, discussions and editing the palaeontological text. We thank C. Reinhard, G. Love, A. Mix, J. Morford, D. Adams, J. Owens, C. Li and L. Och for discussions and S. Bates, G. Gordon and J. Owens for assistance with laboratory analyses. We thank M. Wille for comments and suggestions.

**Author Contributions** The research was planned by G.J., T.W.L., A.D.A., X.S., S.K.S., N.J.P., B.K. and X.W. Samples were collected by S.K.S., X.W. and G.J. The manuscript was prepared by S.K.S., N.J.P. and G.J., with important contributions from all co-authors. Analyses were carried out by S.K.S. with contributions from N.J.P. and B.K.

**Author Information** Reprints and permissions information is available at [www.nature.com/reprints](http://www.nature.com/reprints). The authors declare no competing financial interests. Readers are welcome to comment on the online version of the paper. Correspondence and requests for materials should be addressed to G.J. (Ganqing.Jiang@unlv.edu).